Differences between the Pressure- and Temperature-Induced Denaturation and Aggregation of β-Lactoglobulin A, B, and AB Monitored by FT-IR Spectroscopy and Small-Angle X-ray Scattering

Gunda Panick, Ralf Malessa, and Roland Winter*

Department of Chemistry, Physical Chemistry I, University of Dortmund, Otto-Hahn-Strasse 6, D-44221 Dortmund, Germany

Received December 1, 1998

ABSTRACT: We examined the temperature- and pressure-induced unfolding and aggregation of β-lactoglobulin (β-Lg) and its genetic variants A and B up to temperatures of 90 °C in the pressure range from 1 bar to 10 kbar. To achieve information simultaneously on the secondary, tertiary, and quaternary structures, we have applied Synchrotron small-angle X-ray diffraction and Fourier transform infrared spectroscopy. Upon heating a β-Lg solution at pH 7.0, the radius of gyration R_g first decreases, indicating a partial dissociation of the dimer into the monomers, the secondary structures remaining essentially unchanged. Above 50 °C, the infrared spectroscopy data reveal a decrease in intramolecular β-sheet and α-helical structures, whereas the contribution of disordered structures increases. Within the temperature range from 50 to 60 °C, the appearance of the pair distance distribution function is not altered significantly, whereas the amount of defined secondary structures declines approximately by 10%. Above 60 °C the aggregation process of 1% β-Lg solutions is clearly detectable by the increase in R_g and intermolecular β-sheet content. The irreversible aggregation is due to intermolecular S−H/S−S interchange reactions and hydrophobic interactions. Upon pressurization at room temperature, the equilibrium between monomers and dimers is also shifted and dissociation of dimers is induced. At pressures of approximately 1300 bar, the amount of β-sheet and α-helical structures decreases and the content of disordered structures increases, indicating the beginning unfolding of the protein which enables aggregation. Contrary to the thermal denaturation process, intermolecular β-sheet formation is of less importance in pressure-induced protein aggregation and gelation. The spatial extent of the resulting protein clusters is time- and concentration-dependent. The aggregation of a 1% (w/w) solution of A, B, and the mixture AB results in the formation of at least octameric units as can be deduced from the radius of gyration of about 36 Å. No differences in the pressure stability of the different genetic variants of β-Lg are detectable in our FT-IR and SAXS experiments. Even application of higher pressures (up to 10 kbar) does not result in complete unfolding of all β-Lg variants.

A. H. Palmer was the first who isolated bovine β-lactoglobulin (β-Lg) (*1*). β-Lg is a major component of whey in milk from many mammals and, because of its gelling abilities, one of the most important proteins in food chemistry. The biological function of the protein is still unclear, although a variety of experiments reveal that the native protein is capable of binding small hydrophobic molecules such as vitamin A, retinol, or fatty acids. The β-Lg monomer is a globular protein of 162 residues (18.3 kDa molecular mass), containing two disulfide bonds and a free cysteine, and consists of antiparallel β-sheets formed by nine β-strands. The crystal structure exhibits that the monomer consists predominantly of β-sheets (50%) and a small proportion of α-helical (15%), random (15%), and turn structures (20%) (*2, 3*).

Aqueous solutions of β-Lg have been extensively studied since the early fifties using many available experimental techniques, such as differential scanning calorimetry (DSC) (*4, 5*), optical rotatory dispersion (ORD) and circular dichroism (CD) (*6*−*8*), light scattering (LS) (*9*), nuclear magnetic resonance NMR (*10*), small-angle X-ray scattering (SAXS) (*11, 12*), and Fourier transform infrared spectroscopy (FT-IR) (*8, 13*). These experimental techniques monitor different structural and physicochemical properties of the protein in solution, and many contradictory results concerning the denaturation and gelation behavior of the protein have been published. Furthermore, the existence of several genetic variants (six at all), among which A and B are the most common ones, with different stability in solution, and the fact that many parameters, such as temperature, thermal history, pH, ionic strength, and protein concentration itself have a significant influence, has complicated the examination of the denaturation process.

The A and B variants of β-Lg differ only at two positions, amino acid 64 and 118, which are Asp and Val for β-Lg A and Gly and Ala for β-Lg B (*14, 15*). The presence of the Asp in β-Lg A means that this variant is more negatively charged than β-Lg B. The isoelectric point of β-Lg is around 5.2 and slightly higher for the B variant than the A variant (*15*).

At pH values between about 5 and 8 the dimer is the most stable aggregate at room temperature, although small proportions of higher aggregates (e.g., tetramers) may be present

* To whom correspondence should be addressed.

10.1021/bi982825f CCC: $18.00
Published on Web 04/27/1999

as well. The attracting forces between the single monomers seem to be weak and of hydrophobic nature. It has been shown by the DSC measurements that at higher protein concentrations β-Lg A is the less stable variant, whereas at low protein concentrations the opposite is found.

Although there appears to be some disagreement about structural changes of the protein upon denaturation, some basic properties of the denatured protein seem to be clear. Upon denaturation the protein does not unfold completely and a considerable amount of secondary structure is retained. Some researchers propose the occurrence of a molten globule (*16*) or the existence of two or more intermediate species during the temperature-induced denaturation (e.g., refs *17*, *18*). From a molecular point of view the role of intermolecular disulfide bonds and the participation of hydrophobic interactions to the thermal aggregation and gelation process were discussed (*18*, *19*). The S−H/S−S interchange reaction seems to play an important role in the aggregation mechanism of β-Lg. Heating of a higher concentrated (>1% (w/w)) (*16*) protein solution results in the formation of a gel with fractal-like properties.

We used also pressure as a variable to establish experimental conditions under which a different mechanism of aggregation might occur. It has long been known that the application of hydrostatic pressure results in the disruption of native protein structure (*20*, *21*) due to the decrease in the volume of the protein−solvent system upon unfolding. Pressure denaturation studies thus provide a fundamental thermodynamic parameter for protein unfolding, the volume change $\Delta V°$. A number of reviews on effects of pressure on proteins discuss these volume changes in greater detail (*22*−*26*). The pressure-induced denaturation and aggregation process of β-Lg B and AB has been investigated using experimental techniques such as fluorescence, CD, SDS−PAGE, and rheology (*27*−*30*). In this paper we report on the pressure- and temperature-induced changes in the quaternary, tertiary, and secondary structures of β-Lg A, B, and AB characterized by SAXS and FT-IR spectroscopy. These studies provide a picture of the extent of compactness and secondary structure which occurs during temperature- and pressure-induced unfolding and aggregation/gel formation of β-Lg. A basic challenge in the study of pressure effects on proteins is to understand the mechanisms of pressure unfolding (*31*), hydration, dissociation/aggregation, and gelation under pressure. Another challenge concerns the use of applying high pressure for processing protein-rich foods and food products, especially in the dairy field (e.g., refs *32*−*34*). Pressure-induced gelation of proteins has attracted a considerable interest mainly because high-pressure-processed food retains the sensory and nutritional properties of the fresh product, and also because the gels thus formed have unique textures. (*35*, *36*).

MATERIALS AND METHODS

Bovine β-Lg A, B, and AB were purchased from Sigma and used without further purification.

The small-angle X-ray scattering (SAXS) experiments were performed at the X13 beamline of the EMBL outstation at DESY in Hamburg (*31*, *37*, *38*). The synchrotron radiation was monochromatized by a silicon monochromator resulting in a fixed wavelength of $\lambda = 1.5$ Å. A camera length of 3.2 m was used which covers a wide range of momentum transfers Q [$Q = (4\pi/\lambda)\sin\theta$; λ wavelength of radiation, 2θ scattering angle], from 0.02 to 0.2 Å^{-1}. The small-angle scattering was recorded using a position-sensitive linear detector (*39*). The detector was calibrated using dry rat tail tandon which has a long spacing of 640 Å. For the high-pressure measurements we used a home-built thermojacketed high-pressure cell with flat type IIa diamonds (6 mm diameter, 0.8 mm thickness) as window material and water as pressure transmitting medium. The pressure was measured with a precision strain gauge pressure transducer (SENSOTEC, model UHP/721-03). The maximum uncertainty associated with the pressure determination is estimated as ±10 bar. Temperature was controlled using a water bath and a thermocouple inserted into a hole drilled into the high-pressure cell body. All pressure measurements were performed at 20 ± 1 °C. Unless otherwise stated, a protein concentration of 10 mg/mL was chosen. With this protein concentration, typical exposure times were, due to the highly absorbing window material, 40 min for the pressure and 5 min for the temperature-dependent measurements. The pressure measurements were performed in 10 mM Tris buffer solution adjusted to pH 7.0. For the temperature-dependent scattering experiments the sample in 10 mM phosphate buffer at pH 7.0 was allowed to equilibrate 15 min prior to data collection at the temperature chosen. After subtraction of the background scattering using the pure buffer solution data, taking into account the pressure-dependent absorption factors, data evaluation of the SAXS measurements was performed using the indirect Fourier transformation method (*40*−*42*). We have used SAXS to probe the overall conformation of the protein by measuring its radius of gyration and pair distance distribution function $p(r)$, which are sensitive to the spatial extent and shape of the particle. The square of the radius of gyration R_g of the scattering particle is obtained from the normalized second moment of $p(r)$

$$R_g^2 = \frac{\int_0^{R_{max}} p(r) r^2 dr}{2\int_0^{R_{max}} p(r) r dr} \quad (1)$$

The pair distance distribution function $p(r)$ is given by the Fourier transform of the measured scattered intensity $I(Q)$

$$p(r) = \frac{1}{2\pi^2}\int_0^{\infty} I(Q) Qr \sin(Qr) dQ \quad (2)$$

For a particle with uniform electron density, $p(r)$ is the frequency of vector lengths r connecting small volume elements within the volume of the scattering particle with maximum dimension R_{max}.

Fourier transform infrared (FT-IR) spectra were recorded with a Nicolet Magna 550 spectrometer equipped with a liquid nitrogen cooled HgCdTe detector. For the pressure-dependent measurements the infrared light was focused by a spectra bench onto the pinehole of the diamond anvil cell (*31*, *43*). Each spectrum was obtained by coadding 512 scans at a spectral resolution of 2 cm^{-1} and was apodized with a Happ-Genzel function. The spectrometer and sample chamber were continuously purged with dry and carbon dioxide-free air. Powdered α-quartz was placed in the hole of the steel gasket, and changes in pressure were quantified by the

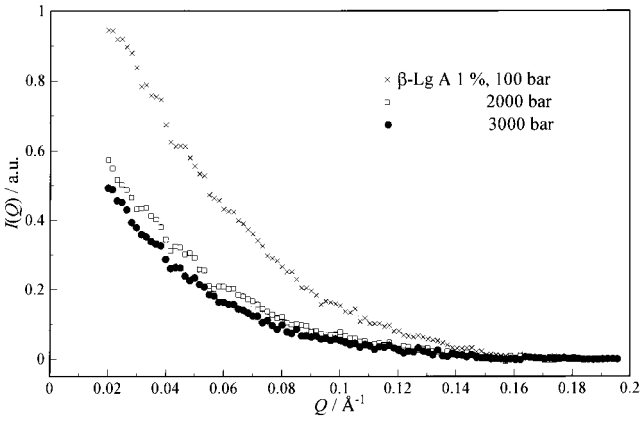

FIGURE 1: Synchrotron X-ray small-angle scattering patterns of β-Lg A (1% (w/w)), in the diamond cell at 20 °C and three selected pressures.

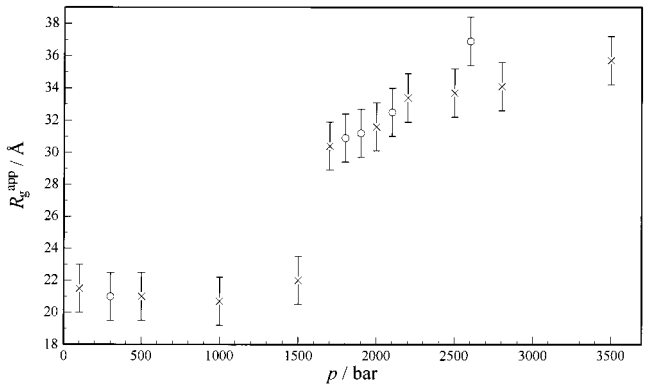

FIGURE 2: Apparent radius of gyration R_g of β-Lg A (1% (w/w), pH 7, Tris buffer) as a function of pressure ($T = 20$ °C; the different symbols are for different runs).

shift of the quartz phonon band at 695 cm^{-1} (*44*). The thermal denaturation was measured using a cell with CaF_2 windows separated by 25 μm Teflon spacers. An external water thermostat was used for pressure- and temperature-dependent measurements to control the temperature within 0.1 °C.

Fifty milligrams of protein was dissolved in 1 mL of D_2O buffer containing 50 mM Tris (pH 7.0). The pK_a of Tris is pressure-insensitive since both the acid and base forms exhibit the same charge, thus eliminating electrostriction effects associated with deprotonation. To ensure complete H−D exchange, we heated the protein solution to 45 °C for 1 h and then stored it overnight at room temperature.

Fourier self-deconvolution (FSD) was performed with a resolution enhancement factor (K value) of 1.8 and a bandwidth (full width at half height) of 15 cm^{-1}, over the wavenumber range 1520−1720 cm^{-1}. The fractional intensities of the secondary structure elements were calculated from a band-fitting procedure assuming a Gaussian−Lorentzian line shape function (*45*, *46*). The reproducibility of the data is well within the given error limits (5%). The relative accuracy is much better, however.

SAXS RESULTS

We have used small-angle X-ray scattering (SAXS) to probe the temperature and pressure dependence of the tertiary and quaternary structures of the different genetic variants of β-Lg in aqueous solution. In the pH range from 5.0 to 7.5 at room temperature, for the genetic variants A and B, the β-Lg dimer (36 kDa) is the most stable species in solution (*47*). As it has been found in other experiments (*18*) the β-Lg sample obtained by Sigma Chemicals is inhomogeneous in composition and contains sometimes a significant amount of protein aggregates higher than dimeric. This may be caused by aggregation during the industrial isolation process. The fact that SAXS is very sensitive to the averaged spatial extent of the protein aggregate in solution has led to differences in the R_g^{app} of the native protein in certain samples at ambient pressure and temperature. Although higher aggregates are sometimes found in solution, the basic features of the unfolding and denaturation, such as, the onset temperature, remain similar to those of the dimeric protein. In this paper only measurements with an initial radius of gyration close to the native dimeric protein are shown.

Pressure-Induced Denaturation. Figure 1 shows the background-subtracted small-angle X-ray scattering data of a 1% (w/w) solution of β-Lg A at selected pressures. At pressures above 1500 bar a significant change in the SAXS pattern is observed. The pressure-induced changes in the scattering contrast between the protein and the buffer solution result in a decrease of the protein scattering intensity at higher pressures. We used the normalized second moment of the pair distance distribution function $p(r)$ to obtain the apparent radius of gyration R_g^{app} of β-Lg (eq 1). Figure 2 exhibits the pressure-induced change in the radius of gyration of a 1% (w/w) solution of β-Lg A in 10 mM Tris buffer solution at pH 7.0. At room temperature (20 °C) and ambient pressure, R_g^{app} is 21 ± 1.5 Å. This value is within the experimental error the radius of gyration of the dimeric form of β-Lg, which can be calculated (*48*) from the crystal structure (21.48 Å) and which is also found in the literature (*11*, *49*). With increasing pressure, R_g^{app} seems to decrease slightly. This decrease is within the indicated error bars of the experiment, however. It may be caused by a partial dissociation of the dimers. At pressures above 1500 bar the radius of gyration increases, and at 3500 bar a value around 36 ± 1 Å is found. This behavior of $R_g^{app}(p)$ is similar for both genetic variants, A and B, and also for the mixture of A and B (data not shown). In the pressure range from 1 to 1500 bar, a small proportion of the dimers probably dissociates and this dissociation is followed by an essentially irreversible aggregation process. The radius of gyration of 36 Å at high pressures is similar to the R_g^{app} which is typical for an octameric cluster of β-Lg, $R_g = 34.4$ Å (*9*). The pressure-induced unfolding and denaturation is only partially reversible.

Figure 3 exhibits the pair distance distribution function $p(r)$ of β-Lg A as a function of pressure at 20 °C. In the native state at ambient pressure, $p(r)$ can be interpreted as a distance distribution function of an ellipsoidal particle with a maximum dimension around 55 Å. Upon pressurization above 1500 bar, the maximum dimension R_{max} of the object increases approximately 2-fold, to about 110 Å at 3500 bar. It can be deduced from the extrapolated scattering intensity $I(Q)$ at $Q = 0$, which is proportional to the molecular mass of the aggregate and increases above 1500 bar, that the increase in the maximum dimension of the particle is caused by a denaturation-induced aggregation process. A more detailed interpretation of the $p(r)$ function is difficult because of the polydispersity of the sample. The resulting R_g^{app} of 36

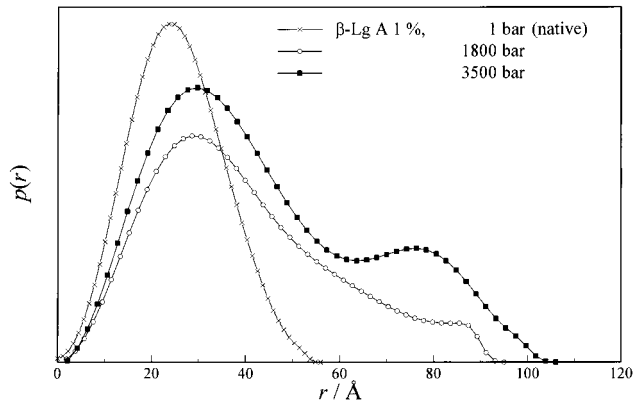

FIGURE 3: Pair distance distribution function $p(r)$ of β-Lg A (1% (w/w)) at selected pressures ($T = 20$ °C).

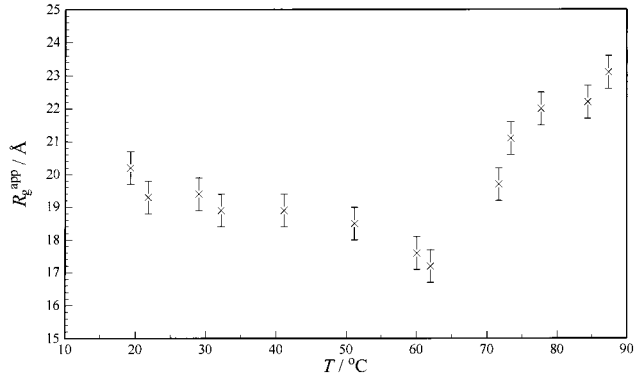

FIGURE 4: Apparent radius of gyration R_g of β-Lg A as a function of temperature at ambient pressure.

Å implies that clusters as large as octameric units are formed. In the time limit of our measurements (approximately 1 h), no significant amount of larger aggregates can be found. Prolonged pressurization leads to an increase of the apparent radius of gyration, however.

Within the experimental errror of the SAXS experiment no differences in the pressure-induced denaturation and aggregation behavior of β-Lg A, B, and the mixture AB can be found. Pressure denaturation of higher concentrated β-Lg samples (>2% (w/w)) results in a largely irreversible formation of a gel-like structure. The extent of aggregation is a function of the protein concentration, applied pressure, and the buffer system (*27*, *50*).

Temperature-Induced Denaturation. Heating of a 10 mM phosphate buffer solution of β-Lg A (1% (w/w)) to temperatures above 60 °C results in denaturation and aggregation of the protein. At room temperature and ambient pressure the R_g^{app} of the protein is 19.5 Å. The slight difference in the radius of gyration to the pressure-dependent measurements shown above may be due to the different buffer system. The amount of monomeric units appears to be higher in the phosphate buffer solution. The pH of Tris buffer solution is insensitive to pressure effects over a wide range of pressures, but the pH of Tris buffer varies slightly with temperature. Upon heating, R_g^{app} decreases to approximately 18 Å at 60 °C, and above 62 °C it increases due to partial unfolding and the formation of larger aggregates is induced (Figure 4). The resulting radius of gyration is time- and concentration-dependent. Heating of a higher concentrated β-Lg solution results in the formation of larger clusters and in gelation. A Kratky representation of the scattering data of a

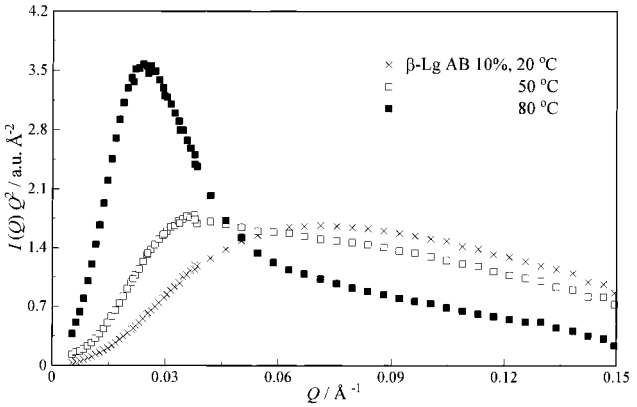

FIGURE 5: Kratky plots of β-Lg A (10% (w/w)) at selected temperatures ($p = 1$ bar).

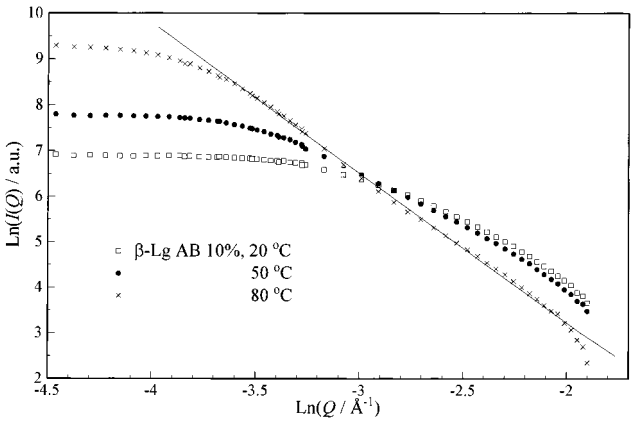

FIGURE 6: Ln-ln plot of the small-angle scattering intensity $I(Q)$ of β-Lg AB (10% (w/w), pH 7.0) at selected temperatures ($p = 1$ bar).

10% (w/w) solution of β-Lg AB reveals the formation of large globular particles at high temperatures (Figure 5). Determination of the Porod slope for the temperature-induced gel state of this highly concentrated protein solution exhibits the formation of aggregates with fractal-like scaling behavior (*51*) (Figure 6). The change in the slope of the ln-ln plot of the scattering intensity $I(Q)$ exhibits a crossover in the scattering behavior of the aggregating protein. At 80 °C the slope of -3.3 indicates the formation of a surface fractal with a fractal dimension of 2.7. A detailed interpretation of this fractal dimension is difficult, however. The cutoff dimensions for the fractal-like structure of the aggregate are approximately only 50 and 250 Å.

A difference in the thermal stability of the single genetic variants and the mixture is the starting temperature for the denaturation or aggregation process. The onset is estimated from the first increase in R_g^{app}. For an A and B mixture of β-Lg the onset occurs at about 62 °C, for A at about 65 °C, and for B at about 70 °C. The increase in stability for the B variant, as can be deduced from the higher aggregation temperature, is in accordance with results from other experimental methods (*52*).

FT-IR RESULTS

To analyze the pressure- and temperature-induced changes in the secondary structure of β-Lg, we concentrated on the carbonyl stretching vibration, the amide I′ region of the infrared spectrum. The FT-IR spectrum exhibits a broad band

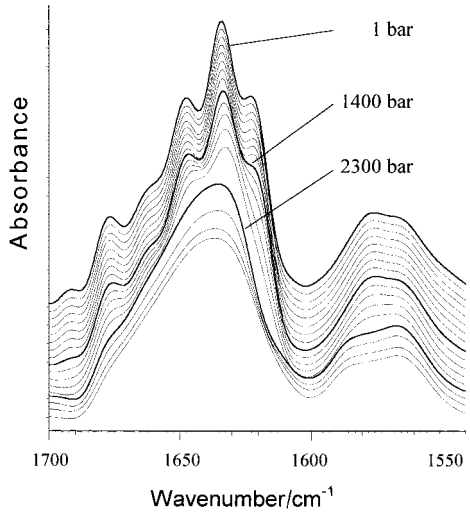

FIGURE 7: Deconvoluted FT-IR absorption spectra of β-Lg A at 20 °C as a function of pressure.

contour between 1600 and 1700 cm^{-1} which is due to overlapping bands of different secondary structure elements. It is primarily (about 80%) due to the C═O stretching vibrations of the protein backbone. The wavenumber of the amide I vibration is determined by the nature of the hydrogen bonds involving the C═O and N—H groups of the peptide linkage and the geometry of the protein backbone and, thus, is sensitive to changes involving the secondary structure of proteins. Even marginal changes in protein conformation are detectable (*56*). Variations in the length and direction of hydrogen bonds result in variations of the strength of the hydrogen bond for different secondary structures, which in turn produces characteristic electron densities in the amide C═O groups, resulting in characteristic amide frequencies. The stronger the hydrogen bond involving the amide C═O, the lower the electron density in the C═O group and the lower the amide I absorption frequency appears.

To resolve these bands, we use the Fourier self-deconvolution technique. The assignment of the components for β-Lg is based on previous studies (*8*, *13*, *53*−*56*). The band at 1634 cm^{-1} corresponds to intramolecular β-sheet structures, and the absorption around 1624 cm^{-1} is associated with exposed β-sheets (for example β-strands with strong hydrogen bonding that are not part of the core of β-sheets). The multiplicity of band frequencies observed reflects differences in hydrogen bonding strength as well as differences in transition dipole coupling in different β-strands. Bands at about 1624 and 1684 cm^{-1}, when coupled, are associated with aggregated, intermolecular β-sheets (β-aggregation), which occur at elevated temperatures. The IR absorption band at 1645 cm^{-1} is assigned to disordered structures, whereas the bands at 1664 and 1677 cm^{-1} are caused by turn structures. The band at 1652 cm^{-1} is due to α-helices, and side chain vibrations (C═C stretching vibrations) of aromatic amino acid residues occur arround 1610 cm^{-1}.

Pressure-Induced Denaturation. Figure 7 shows the deconvoluted FT-IR spectra of β-Lg A as a function of pressure at ambient temperature. In the spectrum of the native protein the maximum at 1634 cm^{-1} and the shoulder arround 1624 cm^{-1} reflect a high β-sheet content, while the band at 1652 cm^{-1} is due to the relatively low α-helical content. The pressure-dependent data reveal a conformational transition

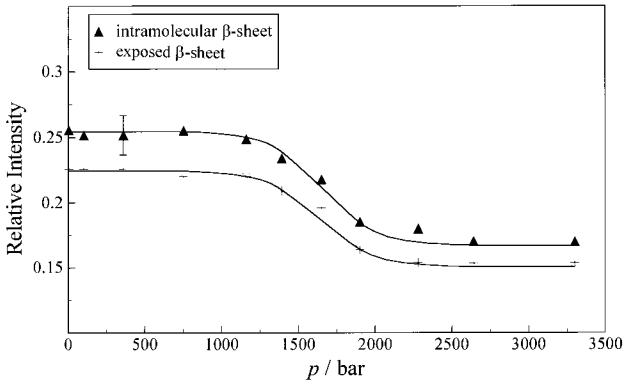

FIGURE 8: Pressure effect on the areas of the bands associated with β-sheet structures of β-Lg A (T = 20 °C).

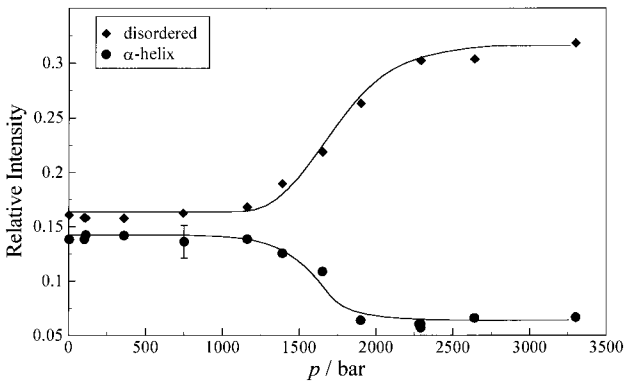

FIGURE 9: Pressure effect on the areas of the bands associated with α-helical and disordered structures of β-Lg A (T = 20 °C).

in the secondary structure of β-Lg A between 1.4 and 2.5 kbar indicated by the disappearance of the spectral fine structure. In the deconvoluted FT-IR spectra for pressures above 2.5 kbar, only one broad band appears, with a maximum at 1640 cm^{-1} indicating the formation of a higly disordered protein structure. The spectra of β-Lg B and AB acquired under the same conditions are similar (data not shown).

Figures 8 and 9 exhibit the changes in the fractional intensities of bands assigned to the different secondary structure elements. Fits of the FT-IR spectrum for native β-Lg obtained at ambient temperature and pressure in terms of the relative contributions of the various secondary structural elements agree reasonably well with the X-ray results (*57*) in view of an approximately 5% error of the FT-IR method. The fits reveal the same secondary structure content for β-Lg A and B under native conditions, confirming the results of the FT-IR study of Dong et al. (*8*). The pressure-induced denaturation of β-Lg A at pH 7.0 is accompanied by an increase in the fractional band intensity of disordered structures, while the intensity of the absorption bands associated with β-sheets and α-helices decreases. Although the fractional intensity of β-sheets decreases significantly, the β structures are not completely disrupted by pressure up to 3.3 kbar. β-Lg B and AB reveal a similiar pressure-induced denaturation behavior (data not shown). The secondary structural compositions estimated by the fits thus indicate that no significant difference in the resulting secondary structure of the genetic variants A, B, and AB occurs upon pressurization.

Temperature-Induced Denaturation. Figure 10 shows the deconvoluted, temperature-dependent FT-IR spectra of β-Lg

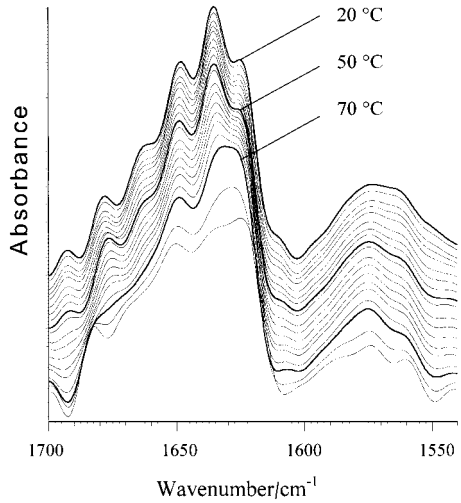

FIGURE 10: Deconvoluted FT-IR absorption spectra of β-Lg A as a function of temperature at ambient pressure.

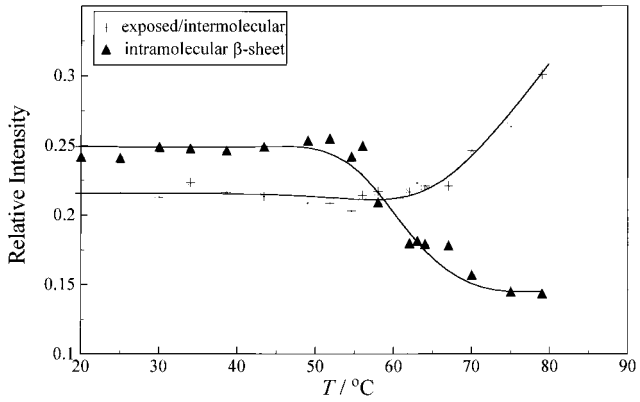

FIGURE 11: Temperature effect on the areas of the bands associated with intra- and intermolecular β-sheet structures of β-Lg A (T = 20 °C).

A at ambient pressure. The spectrum of the native protein acquired in the temperature cell is not distinguishable from that obtained in the pressure cell. The temperature-dependent spectra exhibit no significant changes in the amide I′ band below 50 °C. Between 50 and 70 °C, the band maximum shifts toward lower wavenumbers due to the thermal denaturation of β-Lg A. Above 68 °C maxima around 1624 and 1685 cm^{-1} are observed, indicating the formation of intermolecular β-sheet structures, which strongly suggests that thermal aggregation sets in (*54*). The spectra of the genetic variant B reveal a similar transition at temperatures higher than 72 °C and those for β-Lg AB above 65 °C.

For a detailed analysis, the data for the fractional band intensities of the different secondary structure elements are given in Figures 11 and 12 for β-Lg A. The temperature-induced decrease of band intensities linked to intramolecular β-sheets and α-helices is accompanied by an increase in intensities originating from disordered structures. In addition, an increase in band intensity of intermolecular β-sheets occurs above 68 °C (β-Lg B, above 72 °C; β-Lg AB, above 65 °C), indicating the thermal aggregation and gelation process of the protein.

DISCUSSION

Many different models for the thermal denaturation and aggregation behavior of β-Lg have been proposed during

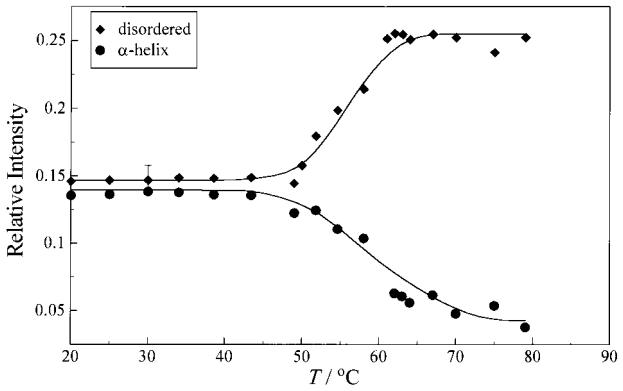

FIGURE 12: Temperature effect on the areas of the bands associated with α-helical and disordered structures of β-Lg A (T = 20 °C).

the last years. One of the first detailed investigations of the temperature-induced denaturation was performed by Stauff and Ühlein (*58*) using light scattering. On the basis of time-dependent changes in the scattered intensity, they proposed a four-state mechanism for the protein denaturation. Their model includes the dissociation of the native protein, association of the subunits to aggregates accompanied with a 2-fold increase in molecular weight, aggregation to tetrameric clusters, and the unspecific aggregation to larger particles. During the following years further experimental approaches led to the development of more complex and detailed denaturation and aggregation models. For example, Griffin et al. (*18*) proposed a mechanism involving a conformational, pH-dependent transition (Tanford transition (*7*)), the dissociation into monomers, and a further conformational change, which is followed by either initial aggregation to rodlike particles or by formation of a denaturated β-Lg species with reduced capability for aggregation. Further heating results in the formation of a fractal-like network structure, the formation of which can be described in terms of a reaction-limited cluster aggregation model.

To achieve information simultaneously on the secondary and quaternary structural levels of β-Lg upon denaturation and aggregation, we examined the temperature- and pressure-induced unfolding and aggregation of β-Lg and its genetic variants A and B. In solution at pH 7.0 the native β-Lg dimer ($R_g \approx 21$ Å) is the most stable species containing a high content of β-sheet secondary structure (ca. 50%), which is in agreement with the crystallographic studies of this protein (*2*, *3*, *57*).

When the solution is *heated* above 30 °C, R_g decreases, indicating a reversible partial dissociation of the dimer into the monomers. Within this temperature range the secondary structure of all β-Lg variants remains essentially unchanged, as shown by the analysis of the infrared spectra. Therefore, in a first step essentially the dissociation of the dimer occurs without a conformational transition of the protein molecule which is in agreement with the results obtained from CD measurements (*18*). No deviations in the dissociation behavior between the variants A and B are detectable. On heating the protein solution above 50 °C, FT-IR spectroscopy data reveal a decrease in intramolecular β-sheet and α-helical structures, while the contribution of disordered structures increases. In low concentrated β-Lg solutions, these temperature-induced changes are not detectable in the small-angle X-ray scattering pattern. On one hand the alterations

in the spatial extent of the single protein molecule should be rather small, which is expected for a native to molten globule type of transition. On the other hand the increase in the radius of gyration should be compensated by the decrease of R_g^{app} due to the partial dissociation of the dimers. Within the temperature interval from 50 to 60 °C, the appearance of the pair distance distribution does not change significantly, whereas the amount of defined secondary structure declines approximately by 10%. Thus, the partial structural changes of the native conformation take place without a significant swelling of the β-Lg molecule. Measurements at higher concentrated protein samples exhibit an increase in the radius of gyration and the changes in the secondary structure content at similar temperatures, however. The pair distance distributions and the Kratky plots reveal a large broadening, indicating the formation of more or less spherical aggregates. For a 10% (w/w) phosphate buffer solution of β-Lg, the aggregation sets in at approximately 48 °C.

It can thus be deduced that at temperatures close to 50 °C the protein monomers unfold in part and thus gain the ability to aggregate at these conditions. The formation of larger clusters depends then on the sticking ability, the time scale of the experiment, and the protein concentration. Above 60 °C the aggregation process of a 1% β-Lg A solution is clearly detectable by the increase in intermolecular β-sheet content and radius of gyration. Cooling the heated sample back to room temperature exhibits only minor changes in the FT-IR absorption spectra and the SAXS patterns, indicating that the aggregation process is mostly irreversible.

Several authors have found that the buried sulfhydryl group is exposed to the solvent upon heating (*16*, *58*). This group promotes S−H/S−S interchange reactions and therefore also the aggregation process. In agreement with other studies (*19*, *59*), the FT-IR experiments reveal a partial unfolding of secondary structures which results in the formation of disordered structures followed by the formation of intermolecular β-sheets. Thus it is most likely that the irreversible cluster formation is due to intermolecular S−H/S−S interchange reactions and to hydrophobic interactions. The fractal dimension of the aggregates formed varies as a function of concentration, thermal history, and buffer. The surface fractal dimension found here at pH 7.0 is 2.7.

The examination of *pressure* effects on the unfolding reaction and gelation behavior of β-Lg was guided by the relative importance of β-Lg in food processing and, at least in part, by the possibility to extract β-Lg from whey by means of high pressure. Pressure affects the monomer−dimer equilibrium of native β-Lg in 10 mM Tris buffer solution at pH 7.0 in a way similar to that of temperature increase. Upon pressurization to 1500 bar, the equilibrium between monomers and dimers is probably shifted and partial dissociation of dimers is induced. The amount of dissociation seems to be smaller than that induced by temperature. The dissociation is caused by the pressure-induced destabilization of hydrophobic interactions, a well-known fact in high-pressure protein chemistry (*24*, *60*). The pressure-induced dissociation into monomers is accompanied by conformational changes of secondary structure. At pressures of approximately 1300 bar, the IR absorption bands assigned to intramolecular β-sheets and α-helical structures decrease while the content of disordered structures increases, indicating a beginning unfolding of the protein which enables aggregation. Contrary to the thermal denaturation, the amount of exposed β-sheets also decreases, which leads probably to the absence of extensive hydrophobic interactions during the pressure-induced aggregation process. No differences in the pressure stability of the different genetic variants of β-Lg are detectable in our FT-IR and SAXS experiments. Even application of higher pressures (up to 10 kbar) does not result in complete unfolding of the protein. Defined secondary structures are retained in all variants, and the total secondary structure content is smaller than that in the temperature-induced denaturated state.

The pressure-induced aggregation process of β-Lg was also studied by Funtenberger et al. (*25*, *60*) using polyacrylamide gel electrophoresis (SDS−PAGE). They conclude that pressure induces the formation of intermolecular S−S bonds. Our FT-IR results show the absence of intermolecular hydrophobic interactions during the pressure application. Thus, one might conclude that in pressure denaturation essentially one aggregation mechanism is operative. The spatial extent of the resulting protein aggregates is time- and concentration-dependent. The aggregation of a 1% (w/w) solution of β-Lg A, B, and the mixture AB results, within the time scale of the experiment (several hours), in the formation of at least octameric clusters as can be deduced from the apparent radius of gyration of about 36 Å.

These differences in temperature- and pressure-induced unfolding and denaturation/aggregation mechanism are expected to lead to different gel structures with different physical properties. Indeed, it has been found (*61*, *62*) that pressure-induced aggregation leads to porous gels in contrast to heat-induced gels which display a finely stranded network. A pressure treatment at 4.5 kbar induces weaker intermolecular or interparticular forces than heating at 87 °C. Furthermore, in contrast to *T* gels, *p* gels exhibit a time-dependent strengthening of protein−protein interactions. It has been proposed that the primary aggregates of β-Lg further aggregate during storage through hydrophobic interactions and disulfide bonds.

ACKNOWLEDGMENT

This work was supported by the Deutsche Forschungsgemeinschaft. We would like to thank Dr. G. Rapp from the EMBL outstation at DESY for this help with the Synchrotron SAXS experiments.

REFERENCES

1. Palmer, A. H. (1934) *J. Biol. Chem. 104*, 359−372.
2. Papiz, M. Z., Sawyer, L., Eliopoulos, E. E., North, A. C. T., Findlay, J. B. C., Sivaprasadarao, R., Jones, T. A., Newcomer, M. E., and Kraulis, P. J. (1986) *Nature 324*, 383−385.
3. Monaco, H. L., Zanotti, G., Spadon, P., Bolognesi, M., Sawyer, L., and Eliopoulos, E. E. (1987) *J. Mol. Biol. 197*, 695−706.
4. Qi, X. L., Brownlow, S., Holt, C., and Sellers, P. (1995) *Biochim. Biophys. Acta 1248*, 43−49.
5. Relkin, P. (1996) *Crit. Rev. Food Sci. Nutr. 36*, 565−601.
6. McKenzie, H. A., and Sawyer, L. (1967) *Nature 214*, 1101−1104.
7. Tanford, C., Bunville, L. G., and Nozaki, Y. (1959) *J. Am. Chem. Soc. 81*, 4032−4036.
8. Dong, A., Matsuura, J., Allison, S. D., Chrisman, E., Manning, M. C., and Carpenter, J. F. (1996) *Biochemistry 35*, 1450−1457.

9. Timasheff, S. N., and Townend, R. (1964) *Nature 203*, 517−519.
10. Molinari, H., Ragona, L., Varani, L., Musco, G., Consonni, R., Zetta, L., and Monaco, H. L. (1996) *FEBS Lett. 381*, 237−243.
11. Witz, J., Timasheff, S. N., and Luzzati, V. (1964) *J. Am. Chem. Soc. 86*, 168−173.
12. Arai, M., Ikura, T., Semisotnov, V., Kihara, H., Amemiya, Y., and Kuwajima, K., (1998) *J. Mol. Biol. 275*, 149−162.
13. Casal, H. L., Köhler, U., and Mantsch, H. H. (1988) *Biochim. Biophys. Acta 957*, 11−20.
14. Braunitzer, G., Chen, R., Schrank, B., and Strangl A. (1973) *Hoppe-Seyler's Z. Physiol. Chem. 354*, 867−878.
15. Elofsson, U. M., Paulsson, M. A, and Arnebrant, T. (1997) *Langmuir 13*, 1695−1700.
16. Qi, X. L., Holt, C., Mcnulty, D., Clarke, D. T., Brownlow, S., and Jones, G. R. (1997) *Biochem. J. 324*, 341−346.
17. Mulvihill, D. M., and Donovan, M. (1987) *Ir. J. Food Sci. Technol. 11*, 43−75.
18. Griffin, W. G., Griffin, M. C. A., Martin, S. R., and Price, J. (1993) *J. Chem. Soc., Faraday Trans. 89*, 3395−3406.
19. Matsuura, J. E., and Manning, M. C. (1994) *J. Agric. Food Chem. 42*, 1650−1656.
20. Bridgman, P. W. (1914) *J. Biol. Chem. 19*, 511−512.
21. Suzuki, K., Miyosawa, Y., and Suzuki, C. (1963) *Arch. Biochem. Biophys. 101*, 225−228.
22. Heremans, K. (1982) *Annu. Rev. Biophys. Bioeng. 11*, 1−21.
23. Weber, G., and Drickamer, H. G. (1983) *Q. Rev. Biophys. 16*, 89−112.
24. Silva, J. L., and Weber, G. (1993) *Annu. Rev. Phys. Chem. 44*, 89−113.
25. Gross, M., and Jaenicke, R. (1994) *Eur. J. Biochem. 221*, 617−630.
26. Mozhaev, V. V., Heremans, K., Frank, J., Masson, P., and Balny, C. (1996) *Proteins: Struct., Funct., Genet. 24*, 81−91.
27. Funtenberger, S., Dumay, E., and Cheftel, J. C. (1997) *J. Agric. Food Chem. 45*, 912−921.
28. Dufour, E., Bon Hoa, G. H., and Haertlé, T. (1994) *Biochim. Biophys. Acta 1206*, 166−172.
29. Tanaka, N., Tsurui, Y., Kobayashi, I., and Kunugi, S. (1996) *Int. J. Biol. Macromol. 19*, 63−68.
30. Van Camp, J., and Huyghebaert, A. (1995) *Food Chem. 54*, 357−364.
31. Panick, G., Malessa, R., Winter, R., Rapp, G., Frye, K. J., and Royer, C. (1998) *J. Mol. Biol. 275*, 389−402.
32. Hayashi, R., and Balny, C., Eds. (1996) *High-Pressure Bioscience and Biotechnology*, Elsevier, Amsterdam, The Netherlands.
33. Balny, C., Hayashi, R., Heremans, K., and Masson, P., Eds. (1992) *High Pressure and Biotechnology*, Vol. 224, John Libbey Eurotext, Colloque Inseram, Montrouge, France.
34. Heremans, K., Ed. (1997) *High-Pressure Research in the Bioscience and Biotechnology*, Leuven University Press, Leuven, Belgium.
35. Dumoulin, M., Ozawa, S., and Hayashi, R. (1998) *J. Food Sci. 63*, 92−95.
36. Kanno, C., Mu, T.-H., Hagiwara, T., Ametani, M., and Azuma, N (1998) *J. Agric. Food. Chem. 46*, 417−424.
37. Rapp, G. (1992) *Acta Phys. Pol., A 82*, 103−120.
38. Czeslik, C., Malessa, R., Winter, R., and Rapp, G. (1996) *Nucl. Instrum. Methods Phys. Res., Sect. A 368*, 847−851.
39. Gabriel, A. (1977) *Rev. Sci. Instrum. 48*, 1303−1305.
40. Glatter, O. (1977) *Acta Phys. Austriaca 47*, 83−102.
41. Glatter, O. (1979) *J. Appl. Crystallogr. 12*, 166−175.
42. Glatter, O., and Kratky, O. (1982) *Small-angle X-ray scattering*, Academic Press, New York.
43. Reis, O., Winter, R., and Zerda, T. W. (1996) *Biochim. Biophys. Acta 1279*, 5−16.
44. Siminovitch, D. J., Wong, P. T. T., and Mantsch, H. H. (1987) *Biochemistry 26*, 3277−3287.
45. Byler, D. M., and Susi, H. (1986) *Biopolymers 25*, 469−487.
46. Prestrelski, S. J., Byler, D. M., and Liebman, M. N. (1991) *Biochemistry 30*, 133−143.
47. Pessen, H., Purcell, J. M., and Farrell, H. M. (1985) *Biochim. Biophys. Acta 828*, 1−12.
48. Svergun, D., Barberato, C., and Koch, M. J. (1995) *J. Appl. Crystallogr. 28*, 768−773.
49. Green, D. W., Aschaffenburg, R., Camerman, A., Coppola, J. C., Dunnill, P., Simmons, R. M., Komorowski, E. S., Sawyer, L., Turner, E. M. C., and Woods, K. F. (1979) *J. Mol. Biol. 131*, 357−397.
50. Renard, D., Lefebvre, J., Griffin, M. C. A., and Griffin, W. G. (1998) *Int. J. Biol. Macromol. 22*, 41−49.
51. Martin, J. E., and Hurd, A. J. (1987) *J. Appl. Crystallogr. 20*, 61−78.
52. Huang, X. L., Catignani, G. L., Foegeding, E. A., and Swaisgood, H. E. (1994) *J. Agric. Food Chem. 42*, 1064−1067.
53. Chirgadze, Y. N., Federov, O. V., and Trushina, N. P. (1975) *Biopolymers 14*, 679−694.
54. Parris, N., Purcell, J. M., and Ptashkin, M. S. (1991) *J. Agric. Food Chem. 39*, 2167−2170.
55. Van Stokkum, I. H. M., Linsdell, H., Hadden, J. M., Harris, P. I., Chapman, D., and Bloemendal, M. (1995) *Biochemistry 34*, 10508−10518.
56. Fabian, H., Schultz, Chr., Naumann, D., Landt, O., Hahn, U., and Saenger, W. (1993) *J. Mol. Biol. 232*, 967−981.
57. Brownlow, S., Cabral, M. H. J., Cooper, R., Flower, D. R., Yewdall, S. J., Polikarpov, I., North, A. C. T., and Sawyer, L. (1997) *Structure 5*, 481−495.
58. Stauff, J., and Ühlein, E. (1955) *Kolloid-Z. 143*, 1−21.
59. Boye, J. I., Ismail, A. A., and Alli, I. (1996) *J. Dairy Res. 63*, 97−109.
60. Hummer, G., Garde, S., García, A. E., Paulaitis, M. E., and Pratt, L. R. (1998) *Proc. Natl. Acad. Sci. U.S.A. 95*, 1552−1555.
61. Dumay, E. M., Kalichevsky, M. T., and Cheftel, J. C. (1994) *J. Agric. Food Chem. 42*, 1861−1868.
62. Dumay, E. M., Kalichevsky, M. T., and Cheftel, J. C. (1998) *Lebensm.-Wiss. Technol. 31*, 10−19.
63. Funtenberger, S., Dumay, E., and Cheftel, J. C. (1995) *Lebensm.-Wiss. Technol. 31*, 10−19.

BI982825F